MULTISPECTRAL IMAGE ANALYSIS FOR BAS-RELIEF AT THE INNER GALLERY OF BAYON TEMPLE

T. Morimoto[a,*], M. Chiba[b], Y. Katayama[c], K. Ikeuchi[a]

[a]Institute of Industrial Science, The university of Tokyo,Japan - (tetsu23*,ki)@cvl.iis.u-tokyo.ac.jp
[b]Graduated School of the Science & Engineering, Waseda University, Japan - mayukochib@fuji.waseda.jp
[c]Tokyo University Agriculture and Technology, Japan - katayama@cc.tuat.ac.jp

Commission VI, WG VI/4

KEY WORDS: Microorganisms, Biodeterioration, Multispectral image, Normalized cuts

ABSTRACT:

At the Bayon temple in Cambodia constructed by sandstone, a study on biodeterioration is one of key tasks of conservation measures for it. Especially, the progress of the deterioration seen in the bas-relief of the inner gallery which was carved the myth world of Hinduism by outstanding description is remarkable. The purpose of this study is to investigate the kind, distribution, and reproductive cycle of biological colonization to discern the relationship with the environment attribute to deterioration and find an effective method to remove them. We assume that some of the microorganisms can be discriminated by detecting the absorbance spectra of photosynthetic pigments in them. We developed a new multispectral imaging system to analyze the spectral information of different microorganisms on the wall's surface. Our system has a wide field of view, low noise, negligible distortion and high resolution enable us to measure the bas-relief in situ. We also developed a segmentation method in order to the spectral image allow to discriminate kind and distribution of microorganisms. Our classification results show the difference in each microorganism's distribution between rainy and dry seasons.

1 INTRODUCTION

Spectral reflectance is inherent in the nature of objects. Different materials have different spectral reflectance. Object analysis based on this fact has been conducted in many fields, such as medical imaging, agriculture, remote sensing, and archaeology, to name a few.

Our Digital Bayon Project (Ikeuchi and Miyazaki, 2007), which have digitized the shape and surface reflectance of the Bayon Temple in the Angkor ruin for preservation and deterioration prevention, needs to determine what kind of microorganisms are present and how widely they exist over the structural surfaces. This involves the analysis of spectral reflection distribution of microorganisms living on the bas-relief of the Bayon Temple.

The microorganisms are one cause of deterioration in the inner gallery of Bayon Temple. Due to deterioration, the detailed bas-reliefs on the walls are losing their shapes. We examine the kind, distribution, and reproductive cycle of the microorganisms to find an effective method to remove them. We assume that some of them can be discriminated by detecting the absorbance spectra of photosynthetic pigments in them, and we find we can calculate absorbance from reflectance.

For the efficient analysis of spectral distribution over an object surface, a two-dimensional spectral image acquisition system is desirable. Traditional spectral cameras provide spectral data only from a limited area, often from a spot. It is difficult, if not impossible, to cover the entire surface of the bas-relief, whose size is 800m x 4m, located in the inner corridor of the temple. This is one of the motivations for us to develop an efficient, handy, and yet high-resolution spectral imaging system. The requirements of the system are: 1) to cover a wide area for efficient measurement to be able to determine distribution of microorganisms, 2) to be able to ignore variations of illumination conditions in dramatic weather changes from bright sunshine to dark squall, and 3) to design a handy system that can be transported to a deep jungle.

We developed a new multispectral imaging system using a Liquid Crystal Tunable Filter (LCTF) (Tominaga and Okajima, 2000), mounted on an automatic pan/tilt platform. Compared to conventional systems, our system has not only high image quality with sufficient spectral resolution but also a wide capturing angle for efficient sampling.

Preservation of cultural assets involves challenges to spectrum measurement. Cultural assets are often in severe outdoor environments, such as the environments of the pyramids in Egyptian desert or the Angkor ruin in Cambodian jungle. In an outdoor environment, wide alterations in the illumination environment often occur quickly. Fixed exposure of a system causes saturation and underexposure. To tackle these problems, we developed a measuring method that can estimate optimum exposures based on noise analysis of the system.

Preservation of cultural assets also needs to determine not only the kinds of microorganisms that exist but also how widely they are spread and how much they mix with each other. This requires us to segment the multispectral images into spatial segments corresponding to the distribution of these microorganisms.

We propose an effective dimension reduction method by using Normalized Cuts (NCuts) (Shi and Malik, 2000), a class of nonlinear dimensional reducers. NCuts methods are widely used as segmentation methods for RGB images in computer vision, but they are not used for multispectral image segmentation in general. NCuts methods are convenient in reducing dimension in a nonlinear manner, and simultaneously segmenting the data. One difficulty in applying NCuts method to our problem is the necessity of a huge memory space $(N \times N)$ for creating an affinity matrix. We solve this issue by applying a local linear approximation (Bishop, 2008), by assuming local linearity on the tangential space of a global manifold space in the high dimension.

The specific contributions of our work are to propose a multispectral image acquisition technique for obtaining panoramic multispectral images, to develop a segmentation method to handle global nonlinear dimensional reduction, and to apply our method to the microorganisim analysis of bas-relief of Bayon temple actually.

The structure of this paper is as follows. Section 2 describes our hardware design for panoramic multispectral imaging and capturing techniques of data acquisition for cultural assets. Section 3 derives a nonlinear dimension reduction method using the "kernel trick" and NCuts method, and applies the NCuts segmentation to a multispectral image. In Section 4, we evaluate our methods. In Section 5, we demonstrate the application for analyzing microorganisms on the bas-reliefs of the Bayon temple. Finally, we conclude the paper in Section 6.

Figure 1: Bayon temple in Cambodia

2 ACQUISITION OF A MULTISPECTRAL IMAGE

We developed a novel multispectral imaging system that has a wide view angle, high image quality, and an accurate spectrum. The system can efficiently measure a target object in an outdoor environment. In subsection 2.1, we describe the hardware construction of our system. In subsection 2.2, we describe the technique for capturing images in an outdoor environment. In subsection 2.3, we describe reconstruction of each band of images having different configurations, and how to stitch a multispectral image.

2.1 Panoramic Multispectral Camera

Our multispectral imaging system has been designed to be a handy system with spectrum accuracy in each pixel with a wide view angle. The system consists of a small monochromatic CCD camera with a liquid crystal tunable filter (LCTF), shown in Fig. 2, mounted on an automatic pan/tilt platform (CLAUS Inc. Rodeon VR head). The LCTF (CRI Inc. Varispec, Bandwidth 7nm) is an optical filter that allows the wavelength of the transmitted light to be electronically adjusted. The monochromatic CCD camera (Sony XCD-X710) with the LCTF mounted can obtain a series of two-dimensional spectral images by repeatedly changing the LCTF's transmittable wavelength with image acquisitions. The captured image has high image quality without distortion. The LCTF capturing system has a narrow field of view because the LCTF is mounted in front of the lens. We compensate for this problem by using an automatic panorama pan/tilt platform. The system captures a wide view multispectral image by synchronizing these three devices efficiently.

2.2 Estimation of Adaptive Exposure in an Outdoor Environment

The optimal exposure time is necessary to be determined in each wavelength due to the two reasons: uneven characteristics and

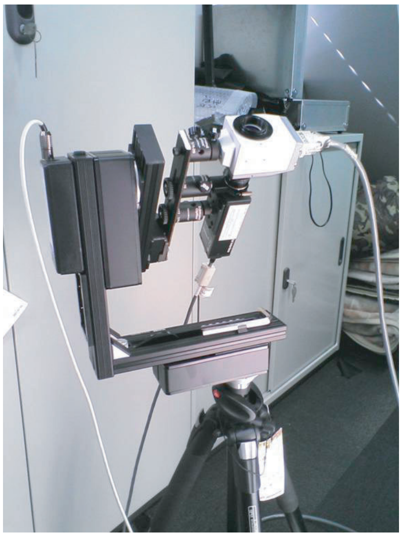

Figure 2: Panoramic multispectral imaging system

varying illumination conditions. A multispectral imaging system using LCTF generally needs a fixed exposure time over the entire range of wavelengths for comparing pixel intensities over all wavelengths. However, the spectral sensitivity given by the combination of LCTF and monochromatic camera is very low in short wavelengths (e.g., 400-500 nm), as shown in Fig. 3.(a), and relatively high in other wavelengths. If the pixel intensity at a certain wavelength would be smaller than the dark current noise, we would not be able obtain a meaningful measurement at that wavelength. For instance, Fig. 3.(b) shows a measured spectrum under dark illumination. Longer exposure time is necessary for spectral accuracy with wavelengths from 400 nm to 500 nm than for other wavelengths.

Varying illumination conditions occur in an outdoor environment, in which many cultural assets are located. Our sensor samples spectral data by changing the LCTF's filtering characteristics and samples a series of images along the wavelengths. During this sampling period, it often occurs that the illumination condition varies due to the movement of clouds. If the intensity of illumination dramatically varies during measurement, it would induce saturation or underexposure at certain wavelengths. The dynamic determination of optimal exposure time at each wavelength is necessary for adjusting the effects of varying illumination conditions.

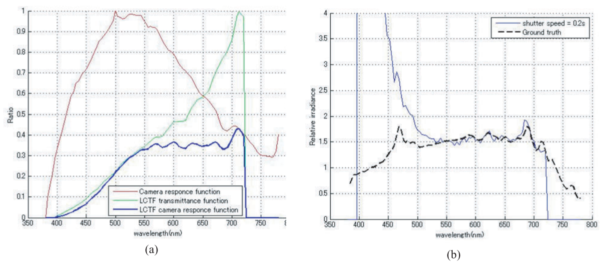

Figure 3: (a) Spectral sensitivity function of monochromatic CCD camera and LCTF transmittance function (b) Illumination spectrum when the exposure time in all bands is fixed.

We attempt to estimate an optimal exposure time for each wavelength based on noise analysis (Reibel et al., 2003). The noise can be categorized into signal-dependent noise (SDN) and signal-independent noise (SIN). In this system, we mainly consider the effect due to the SIN, since the SDN is negligible compared with SIN. The SIN is composed of fixed pattern noise (FPN) and read-out noise, and photo response non-uniformity (PRNU). FPN is a dark current noise, a dynamic component. The read-out noise is composed of the reset noise, amplifier noise, and quantization noise. We focus on the FPN and the read-out noise, since PRNU is a static component easily calibrated in the initial stage.

The FPN depends on the temperature and the exposure time. Here, we assume that the sampling time is reasonably short, say 5 to 10 min, so that the temperature can be considered as constant. The FPN has a linear relation with the exposure time as shown in Fig. 4. a. The linear relation can be expressed as follows: $\epsilon_{DC} = at + b$, where t is an exposure time, a is the amount of the FPN increase depending on exposure times, and b is the amount of the FPN with zero exposure time at that particular temperature. These values are measured at the site before sampling from a series of images with various exposure times while the lens is covered with a cup.

The read-out noise appears randomly at pixel positions at each image. We model the read-out noise as a Gaussian distribution at each pixel. In order to evaluate the parameters of the Gaussian distribution, we obtain a series of lens-covered images, and we calculate mean and standard deviation values. The mean value of images ϵ_{DC} are the FPN, and the standard deviation value of images ϵ_R are read-out noise. We use the upper bound of the SIN as $\epsilon_{DC} + \epsilon_R$.

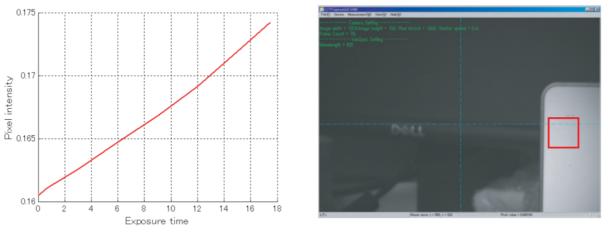

(a) (b)

Figure 4: (a) The correlation between the FPN and exposure time. (b) Captured image of panoramic multispectral imaging system.

Based on the discussion of the noise analysis, we design the procedure to determine the optimal exposure time at each wavelength. The procedure consists of two parts. The first part finds the exposure time that gives the brightest image of a white reference while avoiding saturation over all wavelengths. The second part determines any wavelength that gives lower value in the white reference than the SIN upper boundary, and, if this wavelength exists, it increases the exposure time while avoiding saturation.

The first part consists of:

Step 1. Select the brightest area $(m \times n)$ on a white reference at each wavelength, λ, as shown in Fig. 4. b, and obtain the average brightness within the window, $L(\lambda)$. Repeat this step over all wavelengths

Step 2. Obtain the maximum value, L_{max}, among all the brightness values over all wavelengths.

Step 3. Determine the standard exposure time t_s as the longest exposure time when all the values in the brightest area found in Step 1 are not saturated. Namely, $L_{max} < 2^{16}$.

The second part rescues the particular wavelength image buried under the noise level. For this, we measure the FPN ϵ_{DC} and read-out noise ϵ_R by putting the cap in front of lens. Here, the average value is the FPN, and the standard deviation is considered as the boundary of the read-out noise.

In each wavelength, the optimal exposure time $t(\lambda)$ is adaptively estimated. The optimal exposure time $t(\lambda)$ can be represented as:

$$t(\lambda) = \begin{cases} t_s \frac{\epsilon_{DC}+\epsilon_R+\mu}{L(\lambda)} & (if\ L(\lambda) < \epsilon_{DC} + \epsilon_R + \mu) \\ t_s & (otherwise) \end{cases} \quad (1)$$

where μ is an off-set value to bring the adjustment to the safer side.

2.3 Construction of Panoramic Multispectral Image

After capturing images, we can synthesize the obtained images $L(i,j,\lambda)$ to the spectral power distribution image $L'(i,j,\lambda)$:

$$L'(i,j,\lambda) = t_s \frac{(L(i,j,\lambda) - \epsilon_{DC}(i,j,\lambda))}{t(\lambda)} \quad (2)$$

Here, the FPN image $\epsilon_{DC}(i,j,\lambda)$ in arbitrary exposure time can be estimated by using following equation, according to the linear correlation between the FPN and exposure time, as shown in Fig. 4. a:

$$\epsilon_{DC}(i,j,\lambda) = \alpha(\lambda)\epsilon^s_{DC}(i,j,\lambda) \quad (3)$$

where $\epsilon^s_{DC}(i,j,\lambda)$ is measured as the FPN image first. This can be obtained to calculate the mean image of captured images when light is intercepted from the camera. The linear correlation between the FPN and exposure time is as follows:

$$\alpha(\lambda) = \frac{at(\lambda) + b}{at_s(\lambda) + b} \quad (4)$$

where a and b are, respectively, slope and intercept.

We calculate a spectral power distribution image $L(i,j,\lambda)$, which is divided into the channel values $L'(i,j,\lambda)$ in each pixel i,j by camera sensitivity function $C(\lambda)$, and LCTF transmittance function $T(\lambda)$. Fig. 3 shows the actual sensitivity functions of each.

$$L(i,j,\lambda) = \frac{L'(i,j,\lambda)}{C(\lambda)T(\lambda)} \quad (5)$$

Next, we stitch the multispectral images of different view angles. Stitching usually extracts image features from a pair of images, establishes correspondences among such extracted features, and calculates the translation and rotation parameters to superimpose overlapping areas for connecting these two images. Here, the features in multispectral images are different in each band image. To overcome this issue, we generate an intensity image using all the spectral images in each viewing direction. Second, we extract Scale-Invariant Feature Transform (SIFT) features (interest points) (Lowe, 2004) from these intensity images and establish correspondences for obtaining the translation and rotation parameters. Finally, we stitch the spectral image of each view angle using these parameters. Fig. 5 shows a synthesized panoramic multispectral image.

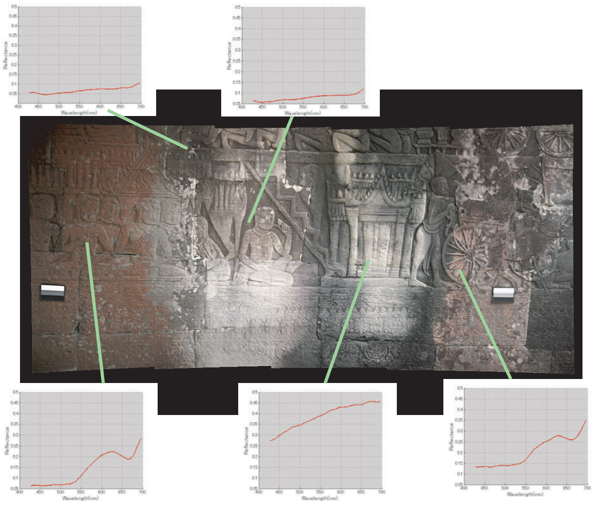

Figure 5: Constructed panoramic multispectral image by proposed system: this image has 81-dimensional spectrum in each pixel.

3 MULTISPECTRAL IMAGE SEGMENTATION

Segmentation of a multispectral image needs dimensional reduction. For dimensional reduction, linear and nonlinear reduction methods exist. Our prime objects, microorganisms on the bas-relief of the Bayon temple, have a nonlinear characteristic in spectral distributions due to the combination of top and bottom layers. This nonlinear problem can be solved either by employing the "kernel trick" such as Kernel PCA (Schölkopf et al., 1998) or extending the Ncut method.

3.1 Nonlinear Mixing

Some of the top layer's pixel spectra typically show mixed spectral characteristics between the top layers and bottom layer. In a remote sensing field, these cause a so-called spectral mixing (Keshava and F.Mustard, 2002). The spectral mixing can be categorized into two models: linear mixing and nonlinear mixing. The linear mixing occurs when one pixel consists of sub-parts from different materials; the different materials are distributed on the image plane. Generally, the linear mixing can be solved by reducing spectral dimension by using PCA, and clustering reduced data.

Our application, analysis of microorganisms, falls in the category of nonlinear mixing. This mixing occurs due to layer surfaces such as microorganisms and bottom rock surfaces. The different half-transparent materials are distributed along the line of sight. The PCA method cannot be applied to nonlinear mixing, but mixing can be achieved either by employing the kernel PCA (KPCA) (Schölkopf et al., 1998) or extending the NCuts method.

3.2 Normalized Cuts

The NCuts method consists of nonlinear dimension reduction and clustering. Among various segmentation methods, the Ncut method has a unique feature of nonlinear dimensional reduction.

For this, let $I = \{I_1, I_2, I_3, ., I_i, .., I_N\}$, where I is input data, of m dimension, at the node i. Then, the NCuts method calculates the weight matrix W, representing similarity among nodes, from the following formula:

$$W_{ij} = exp\left(\frac{-\|I_i - I_j\|^2}{\sigma_I^2}\right) * \begin{cases} exp\left(\frac{-\|X_i - X_j\|_2^2}{\sigma_X^2}\right) & (if\|X_i - X_j\|_2 < r) \\ 0 & (otherwise) \end{cases} \tag{6}$$

where I_i, I_j are input values of m dimensions at the node, i and j, σ_I^2 is the variance of input data, and r is the threshold of the proximity between two nodes in the image. NCuts solves the generalized eigensystem equation:

$$(D - W)y = \lambda D y \tag{7}$$

Next, the Laplacian matrix, $\mathcal{L} = (D - W)$ can be calculated from the weight matrix, W. The normalized Laplacian matrix $\tilde{\mathcal{L}}$ is given by:

$$\tilde{L} = D^{-\frac{1}{2}} L D^{-\frac{1}{2}} = I - D^{-\frac{1}{2}} W D^{-\frac{1}{2}} \tag{8}$$

where D is $N \times N$ diagonal matrix $D_j = diag(W(1, j), W(2, j) \ldots)$, $j = 1, 2, \cdots, N$, and W is $N \times N$ a symmetric matrix $W(i, j) = W(j, i)$. We can transform Eq. 8 into the standard eigensystem as follows:

$$D^{-1/2} W D^{-1/2} z = (1 - \lambda) z \tag{9}$$

We can span a low dimensional space, of E dimensions, with the eigenvectors from the $E + 1$ least significant eigenvalues, where E is the partition number, and we ignore the least significant eigenvalue and the corresponding eigenvector. In the least significant space, all the input data have roughly same values due to the data normalization. We map the input data onto this low dimensional space.

$$y_{E_{ij}} = \frac{z_{i+1,j}}{\sqrt{D_{jj}}}, \quad (i = 1, ..., E + 1, j, ..., N) \tag{10}$$

Finally, we can segment $y_{E_{ij}}$ into E clusters using the k-means method.

3.3 Applying NCuts to multispectral segmentation

Dimensionality is one of the issues in applying the NCuts method to the multispectral image segmentation method. The NCuts method requires making a weight matrix of a high-resolution image, of which the dimensions are $(N \times N)$, where N is the number of image pixels, typically more than 250,000. The NCut method handles this issue by effectively using the proximity threshold, ignoring remote nodes for calculation, and ending up solving a sparse matrix of a high-dimensional image.

We employ a two-step method to overcome this high-dimensional issue. In our microorganism analysis, we cannot apply the proximity threshold because two remotely located regions from the same kind of microorganism should be classified into the same class. We assume that a nonlinear manifold of high dimension has a linear sub-space in a low dimension such as local linear embedding (Roweis and Saul, 2000), or ISOMAP (Tenenbaum et al., 2000). First, we over-segment the multispectral image using a standard PCA method and k-nearest neighbor method, and form super-pixels corresponding to each segment. Then, we apply the NCuts method to these super-pixels.

Our implementation is as follows: First, we compute M super-pixels by over-segmentation using PCA dimension reduction and k-nearest neighbor method. Second, we calculate M mean spectra for all M super-pixels. Let $I = \{I_1, I_2, I_3, ., I_i, .., I_M\}$, where I is spectrum data of m dimensional. Third, we compute the weight matrix W from M $(M < N)$ super-pixel values using the following equation:

$$W_{ij} = exp\left(\frac{-\|I(i) - I(j)\|^2}{t^2}\right) \tag{11}$$

In our experiment, we set t, a normalization factor, at 70% of the maximum distance in the weight graph. Finally, we can segment a multispectral image into material regions by using this weight matrix and NCuts.

4 EXPEIRMENTAL RESULTS

In this section, we describe two experiments. We conducted accuracy verification of Obtained multispectral image. We compared proposed segmentation method with a conventional method.

4.1 Accuracy Verification of Multispectral Image

In this subsection, we evaluate image noise and spectral accuracy of a multispectral image given by our system.

Image Noise Fig. 6. a and b show, respectively, the captured image in fixed exposure, and the captured image by the proposed dynamic exposure method. The captured image from the fixed exposure method provides much noisier data. This effect is more apparent in the short wavelength area. On the other hand, the captured image given by our method is less noisy.

(a) (b)

Figure 6: Image quality of obtained image (a) Captured multispectral image in fixed exposure time. (b) Proposed method.

Spectral Accuracy Table.1 shows the spectral accuracy of our system. In this experiment, we captured multispectral images of a color chart (X-lite Color checker), under artificial sunlight (Seric XC-100), by using both fixed exposure and the proposed dynamic exposure methods, respectively. Then, we measured the spectrum of each patch using a spectrometer (PhotoResearch PR-655) as the ground truth. Second, we calculated the root mean square error (RMSE) between the obtained spectral data and the ground truth in each patch. Compared with the RMSE values by the fixed exposure method, the RMSE values by the proposed method are much lower. The result also showed that our system is effective for spectral analysis.

	RMSE				
Color	Fix	AE	Color	Fix	AE
DarkSkin	4.469	1.301	YellowGreen	0.914	0.764
LightSkin	1.347	1.064	OrangeYellow	0.915	0.870
BlueSky	1.254	0.909	Blue	0.627	0.398
Foliage	3.060	0.850	Green	1.204	0.657
BluishFlower	1.196	0.885	Red	0.953	0.887
BluishGreen	0.916	0.516	Yellow	1.102	0.914
Orange	1.460	0.987	Magenta	1.002	0.885
PurplishBlue	1.420	1.074	Cyan	0.619	0.449
ModerateRed	0.937	0.892	White	1.174	0.892
Purple	1.109	1.029	Mean	1.352	0.854

Table 1: Spectral accuracy

4.2 Compared with Conventional Segmentation Methods

We compared conventional segmentation methods with the proposed method. Figs. 7 show the segmentation results of layered surfaces for examining the effect on the nonlinear mixture. The input image is four watercolor pigments painted on a white paper. First, we calculated reflectance spectra from the input multispectral image by using our method. Second, we segmented the reflectance spectra image into different materials using three methods.

(a) (b) (c) (d)

Figure 7: Segmentation results of layered surfaces (a) Input image (b) Method 1: PCA + k-means (c) Method 2: KPCA + k-means (d) Method 3: Proposed method

This image has complex color between the top layers and the bottom layer. Fig.7. b, by Method 1, and c, by Method 2, include significant segmentation error.

5 MULTISPECTRAL IMAGE ANALYSIS FOR BAS-RELIEF

This section describes how we applied our proposed multispectral imaging system and segmentation method to analyze a cultural asset. At the Bayon Temple in Cambodia, microorganisms are one cause of deterioration in the inner gallery. Fig. 8 show the microscope images of microorganisms observed at each spot. Due to deterioration, the detailed bas-reliefs on the walls are losing their shapes. We examined the kind, distribution, and reproductive cycle of the microorganisms to find an effective method to remove them.

Microorganisims perform photosynthesis by absorbing the light of a specific absorbance spectrum via sunlight, so the waveforms of absorbance spectra vary according to the type of photosynthetic pigment in each microorganisim, as shown in Fig. 9. For example, the absorbance spectrum of gleen agle is shown as the linear sum of the absorbance spectra of chlorophyll A and B. And, Cyanobacteria mainly has chlorophyll a and phycocyanins. Based on above understanding, we assumed that some of them could be discriminated by detecting the absorbance spectra of photosynthetic pigments in them, and we found we could calculate absorbance from reflectance.

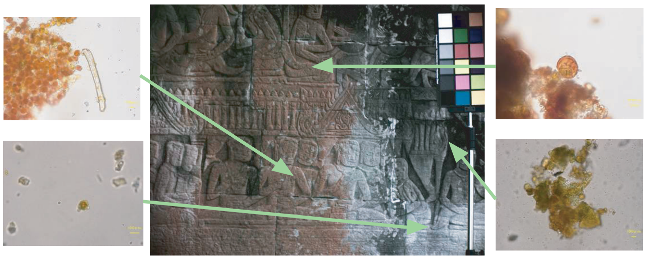

Figure 8: Microbial growth on the wall surface: microscope images of microorganisms observed at each spot.

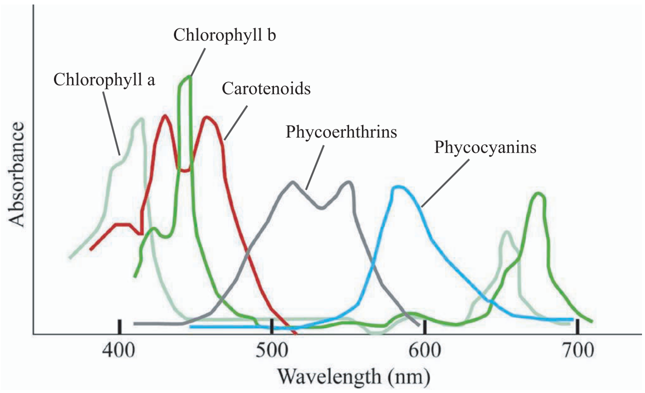

Figure 9: Absorbance of photosynthesis pigments: green algae mainly has chlorophyll a and b. Cyanobacteria mainly has chlorophyll a and phycocyanins.

Fig. 10. a shows the image of the scene we observed. Then, we found correspondences among multispectral images in different seasons to the same area through 3D data.

The results in Fig. 10. b show the measured absorbance spectrum of each segmented area. The three areas, depicted using blue, white, and red colors in the figure, should be differentiated by the quantity of phycocyanin. This is because the areas' absorption has large differences at around 600 nm, which coincides with the phycocyanin's absorbance spectrum as shown in Fig. 9. As Fig. 11 shows, white and blue areas decrease in a dry season compared to a rainy season, which implies that the quantity of phycocyanin has decreased in the dry season. The results indicate that the cyanobacteria, the main source of phycocyanin, increase in a rainy season and decrease in a dry season.

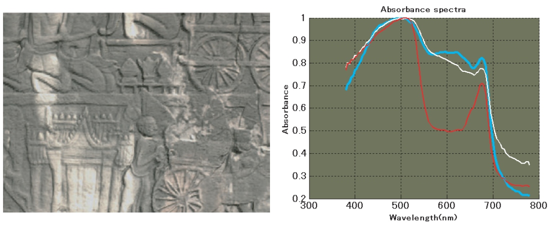

(a) (b)

Figure 10: (a) Observed scene image: this scene was made by mapping a multispectral image onto 3D data. (b) Absorbance spectrum in each class area.

6 SUMMARY

This paper proposed a novel multispectral imaging system and a segmentation method for multispectral images. Our system can efficiently obtain a wide view angle image in an outdoor environment, and also segment a high-dimensional spectral image effectively. In our experimentation, we found that our proposed multispectral imaging system has sufficient accuracy for material segmentation. Furthermore, our multispectral image segmentation method could effectively segment a layered surfaces into different spectra. The system also analyzed microorganisms on bas-reliefs in the Bayon Temple. Our experimental results showed the reproductive cycle of microorganisms in rainy and dry seasons.

Our next task using the proposed system is to consider the relationship between the reproductive cycle of microorganisms and the environment of bas-relief.

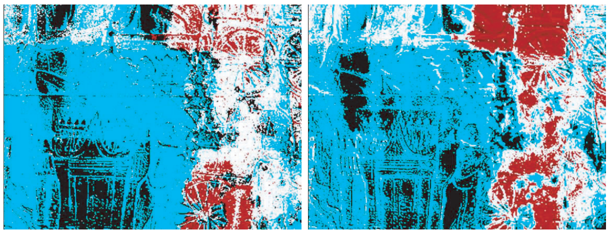

(a) (b)

Figure 11: Segmentation results of microorganisms. (a) Rainy season (b) Dry season

REFERENCES

Bishop, C. M., 2008. Pattern recognition and machine learning. Springer.

Ikeuchi, K. and Miyazaki, D., 2007. Digitally archiving cultural objects. Springer,New York.

Keshava, N. and F.Mustard, J., 2002. Spectral unmixing. IEEE Signal processing magazine.

Lowe, D. G., 2004. Distinctive image features from scale-invariant keypoints. IJCV.

Reibel, Y., Jung, M., Bouhifd, M., Cunin, B. and Draman, C., 2003. Ccd or cmos camera noise charactarisation. The European Physical Journal Applied Physics 21(1), pp. 75–80.

Roweis, S. and Saul, L., 2000. Nonlinear dimensionality reduction by locally linear embedding. Science.

Schölkopf, B., Smola, A. and Müller, K. R., 1998. Nonlinear component analysis as a kernel eigenvalue problem. Neural Computation 10, pp. 1299–1319.

Shi, J. and Malik, J., 2000. Normalized cuts and image segmentation. IEEE Trans. on PAMI.

Tenenbaum, J. B., de Silva, V. and Langford, J. C., 2000. A global geometric framework for nonlinear dimensionality reduction. Science 290, pp. 2319–2323.

Tominaga, S. and Okajima, R., 2000. Object recognition by multi-spectral imaging with a liquid crystal filter. Proc. 15th Int. Conf. on Pattern Recognition.